Deriving the Universal Angular Rate Vector

Russell P. Patera[1]

Abstract

Previous work showed that vehicle attitude propagation accuracy for a slewing angular rate vector can be greatly improved by including the slew rate of the angular rate vector in the propagation algorithm. The improved algorithm employs two sequential rotational increments for each time step. This work presents a method to combine the two rotational increments into a single rotational increment driven by a Universal Angular Rate vector. The Universal Angular Rate vector can be used in the direction cosine and quaternion attitude propagation algorithms to obtain attitude propagation accuracy equivalent to the two rotational increment method. An approximate Universal Angular Rate vector was also derived that avoids the use of trigonometric functions while retaining very high attitude propagation accuracy. Pure coning motion was used to stress test the Universal Angular Rate vector and the approximate Universal Angular Rate vector using direction cosine, linear direction cosine, quaternion, and Bortz propagation algorithms. Results confirmed that by replacing the standard angular rate vector with the Universal Angular Rate vector, attitude propagation accuracy is greatly improved.

Keywords: Attitude propagation, Angular rate vector, Slew rate vector, Coning error, Euler Rotation Vector, Direction cosine matrix

Nomenclature

A	unit vector rotation axis
B	unit vector rotation axis
b	omega plus alpha unit vector
C - I	UAR coefficients
dt	time step
DCM	direction cosine matrix
e_i	axis components
K	z-axis unit vector
q	vector part of quaternion
SRA	slew rate algorithm
U	attitude transformation matrix
UAR	Universal angular rate vector
$\mathbf{X_B}$	body coordinate frame
$\mathbf{X_I}$	inertial coordinate frame
$\boldsymbol{\alpha}$	slew rate of angular rate vector
Δ	integral of angular rate plus alpha
δ	rotation angle increment for SRA
ϵ	axis tilt angle for coning motion

[1] Russell.P.Patera@gmail.com

$\boldsymbol{\Gamma}$	angular increment for UAR
$\boldsymbol{\lambda}$	Universal Angular Rate vector
Ω	integral of slew rate magnitude, α
$\boldsymbol{\omega}$	angular rate vector
ϕ	rotation angle increment for SRA
$\boldsymbol{\theta}$	Euler Rotation Vector

1. Introduction

Vehicle attitude can be propagated using continuous time dependent angular rate vector or a discrete set of angular rotation increments. Each rotation increment is the integral of the angular rate vector over each respective propagation time step. Most attitude propagation algorithms assume that the angular rate vector remains in a fixed orientation during each propagation time step. In typical cases, this assumption is nearly valid, if small enough integration time steps are used. As a result, propagation accuracy is satisfactory. However, the slewing motion of the angular rate vector throughout each time step introduces error, referred to as coning error. If the slewing motion of the angular rate vector is large, coning error can become unacceptable. Coning error can be reduced by increasing the attitude update frequency with associated shorter time steps. The increased update frequency requires increased numerical processing and associated truncation errors that limit the improvement in propagation accuracy. In addition, the increased computer computational load can limit the update frequency and overwork the vehicle's flight computer.

Bortz derived an attitude propagation equation [Bortz, 1971] that was first developed by Laning [Laning, 1949], which involves the Euler Rotation Vector and its time rate of change. Since the rate of change of the Euler Vector can be easily integrated yielding the updated Euler Rotation Vector, attitude propagation can be achieved with a higher update frequency without severe computational load. Bortz's equation is the basis of many numerical algorithms that improve propagation accuracy, which are termed "coning correction algorithms" [Miller, 1983], [Ignagni, 1990], [Ignagni, 1996], [Savage, 1998]. Coning correction algorithms have been implemented in flight computers software to reduce the error in angular rate caused by the vibrational environment experienced by launch vehicles during ascent to orbit. Coning correction algorithms and associated propagation error remains an area of active research. [Xiong, et. al., 2019], [Savage, 2020].

Rather than increasing the attitude update frequency to improve propagation accuracy, an algorithm was developed in previous work [Patera, 2009], [Patera, 2010] that incorporates the slewing angular rate of the angular rate vector into the propagation algorithm. For each propagation time step, two sequential rotational increments about fixed axes are used to achieve attitude propagation. Since each axis has a fixed orientation during each time step, propagation can be achieved without coning error. This propagation algorithm employes larger propagation time steps, lower update frequency and reduced computational load. If the direction of the slew rate of the angular rate vector remains fixed and has a magnitude proportional to the magnitude of the angular rate vector, attitude propagation can be achieved with zero error [Patera, 2011]. Unlike differential equation based propagation algorithms, the propagation time step does not have to be infinitesimal to obtain high accuracy when using the two increment method. Zero propagation error was achieved even with large time steps when stress with pure coning motion [Patera, 2009], [Patera, 2010]. For the case of a general angular rate, use of the algorithm greatly improves attitude propagation accuracy.

The purpose of this work is to derive a Universal Angular Rate vector, UAR, that incorporates the slewing motion of the angular rate vector. The UAR has a fixed orientation throughout each time step and produces a single rotational increment when multiplied by the associated time step. Therefore, by replacing the unmodified angular rate vector with UAR in the direction cosine and quaternion propagation algorithms, both coning and propagation errors are effectively eliminated and high accuracy is achieved. Although UAR eliminates coning error in differential equation based propagation algorithms, it does not eliminate propagation errors caused by finite propagation time steps.

The accuracy of several attitude propagation algorithms associated with different attitude parameterizations were stress tested with pure coning motion. For each algorithm, the error was quantified with a Euler rotation error vector. The attitude error of each algorithm was obtained using the original angular rate vector and compared to the error obtained when UAR was used. The improvement in attitude propagation accuracy was quantified and illustrated graphically.

A conclusion section summarizes the findings of the work.

2. Attitude propagation

Assuming the vehicle has an arbitrary orientation with respect to an inertial reference frame, Euler's Rotation Theorem states that a single rotation of, $\boldsymbol{\theta}$, referred to as the Euler Rotation Vector can bring the body coordinate frame of the vehicle into alignment with the inertial reference frame. Therefore, the orientation of the vehicle can be parameterized with $\boldsymbol{\theta}$. The Direction Cosine Matrix (DCM) given by $\mathbf{U}(\boldsymbol{\theta})$, is a function of $\boldsymbol{\theta}$ and can be used to define the orientation of the vehicle frame with respect to the inertial frame, as given in eq. (1), where the subscripts refer to the body and inertial reference frames.

$$\mathbf{X_I} = \mathbf{U}(\boldsymbol{\theta})\,\mathbf{X_B} \tag{1}$$

If the vehicle has an angular velocity of $\boldsymbol{\omega}$, one can compute the angular rotation increment for a time dt, if we assume that the angular rate remains in a fixed orientation, as shown in eq. (2).

$$\mathbf{d}\boldsymbol{\theta} = \boldsymbol{\omega}\,\mathrm{dt} \tag{2}$$

The associated transformation increment is given by $\mathbf{U}(\mathbf{d}\boldsymbol{\theta})$ and the total transformation is updated by the matrix multiplication given in eq. (3).

$$\mathbf{X_I} = \mathbf{U}(\boldsymbol{\theta})\,\mathbf{U}(\mathbf{d}\boldsymbol{\theta})\,\mathbf{X_B} \tag{3}$$

This process is repeated for each propagation time step, dt, until the final time is reached. Although the angular rate is changing in both magnitude and direction, it is assumed that the direction of the angular rate vector remains fixed throughout each individual increment. In this manner, attitude propagation is achieved using the DCM parameterization of vehicle attitude.

3. Attitude propagation for a slewing angular rate vector

Previous work [Patera, 2009], [Patera, 2010] derived an algorithm for vehicle propagation using the angular rate vector and the slew rate vector of the angular rate vector. Given an angular rate vector of fixed magnitude, $\boldsymbol{\omega}$, that is slewing with a fixed angular rate vector, $\boldsymbol{\alpha}$, the attitude increment for time step, dt, is given by eq. (4). It should be noted that each rotational increment in eq. (4) has fixed orientation and therefore no associated coning error.

$$\mathbf{U}[(\boldsymbol{\omega} + \boldsymbol{\alpha})\mathrm{dt}]\ \mathbf{U}(-\boldsymbol{\alpha}\,\mathrm{dt}) \tag{4}$$

The attitude transformation from the body frame to the inertial frame is found using eq. (4) with eq. (3), as shown in eq. (5).

$$\mathbf{X_I} = \mathbf{U}(\boldsymbol{\theta})\ \mathbf{U}[(\boldsymbol{\omega} + \boldsymbol{\alpha})\mathrm{dt}]\ \mathbf{U}(-\boldsymbol{\alpha}\,\mathrm{dt})\ \mathbf{X_B} \tag{5}$$

This process is repeated for the next time step but with the updated **ω** and **α** in eq. (4). Thus, each attitude increment involves two rotational transformations. The Slew Rate Algorithm, SRA, summarized in eq. (4) and eq. (5) was demonstrated to be highly accurate in previous work [Patera, 2009], [Patera, 2010]. Several methods to obtain the slew rate vector were already published [Patera, 2009], [Patera, 2010] so they will not be repeated in this work.

Additional work [Patera, 2022] extended eq. (4) to a finite propagation time, t, by replacing it with eq. (6), where Δ and Ω are given by eq. (7) and eq. (8). Eq. (6) is valid for **α** remaining in a fixed direction and the magnitude of **ω** being proportional to that of **α**.

$$\mathbf{U}(\mathbf{b}, \Delta)\mathrm{U}(\mathbf{k}, -\Omega) \tag{6}$$

$$\Delta = \int_0^t |\boldsymbol{\omega} + \boldsymbol{\alpha}|\ \mathrm{dt} \tag{7}$$

$$\Omega = \int_0^t |\boldsymbol{\alpha}|\ \mathrm{dt} \tag{8}$$

The angular increment given by **U**(**b**, Δ) is a rotation of Δ about unit vector **b**. The unit vector **b** is aligned with the direction of **ω** + **α** at the beginning of the time increment when t=0. The angular increment given by **U**(**k**, -Ω) is a rotation of -Ω about the unit vector **k**, which is aligned with **α**. Since both **b** and **k** remain in fixed directions throughout the propagation time, coining error is zero. Thus, eq. (6) propagates attitude for a finite propagation time, t, using two rotational transformations, while eliminating coning error. For finite rotations, eq. (6) is used to modify eq. (5), which results in eq. (9).

$$\mathbf{X_I} = \mathbf{U}(\boldsymbol{\theta})\ \mathbf{U}(\mathbf{b}, \Delta)\ \mathrm{U}(\mathbf{k}, -\Omega)\ \ \mathbf{X_B} \tag{9}$$

4. Universal Angular Rate Vector

The goal of this work is to replace the two rotational increments in eq. (4) with a single rotational increment, as shown in eq. (10), where **λ** is the Universal Angular Rate vector replacing **ω**.

$$\mathbf{U}(\boldsymbol{\lambda}\mathrm{dt}) = \mathbf{U}[(\boldsymbol{\omega} + \boldsymbol{\alpha})\mathrm{dt}]\ \mathbf{U}(-\boldsymbol{\alpha}\,\mathrm{dt}) \tag{10}$$

Consider a rotation of δ about the axis **A** followed by a rotation of ϕ about axis **B**, where both **A** and **B** are unit vectors. The combination of these two sequential rotations, yields eq. (11), as derived in an earlier work [Patera, 2017] using Pivot Vectors. Eq. (11) can also be derived using the quaternion composition rule, where **q** is the vector portion of the associated quaternion. The combined rotation has magnitude Γ and is directed in the direction of unit vector **Γ**.

$$\mathbf{q} = \sin\left(\frac{\Gamma}{2}\right)\boldsymbol{\Gamma} = \sin\left(\frac{\delta}{2}\right)\cos\left(\frac{\varphi}{2}\right)\mathbf{A} + \sin\left(\frac{\varphi}{2}\right)\cos\left(\frac{\delta}{2}\right)\mathbf{B} + \sin\left(\frac{\delta}{2}\right)\sin\left(\frac{\varphi}{2}\right)(\mathbf{A}\ \mathrm{X}\ \mathbf{B}) \tag{11}$$

The magnitude of **q** can be computed as the square root of the dot product, as shown in eq. (12) and Γ can be found from q, as given in eq. (13).

$$\mathrm{q} = \mathrm{sqrt}(\mathbf{q} \cdot \mathbf{q}) \tag{12}$$

$$\Gamma = 2 \sin^{-1} \mathrm{q} \tag{13}$$

The rotation vector, **Γ**, of the combined rotation is given by a rotation of Γ about a unit vector in the direction of **q**, as shown in eq. (14).

$$\boldsymbol{\Gamma} = \frac{\Gamma\ \mathbf{q}}{\mathrm{q}} \tag{14}$$

Eq. (11) can be applied to eq. (10) by associating the rotations δ and ϕ with the arguments of **U** in eq. (10), as shown in eq. (15) and eq. (16).

$$\delta\ \mathbf{A} = (\boldsymbol{\omega} + \boldsymbol{\alpha})\ \mathrm{dt} \tag{15}$$

$$\Phi\ \mathbf{B} = -\boldsymbol{\alpha}\ \mathrm{dt} \tag{16}$$

Using eqs. (15) and (16) in eqs. (11 - 13) yields the desired rotation vector in eq. (14). The Universal Angular Rate, **λ**, is found by dividing **Γ** by dt, as given by eq. (17).

$$\boldsymbol{\lambda} = \boldsymbol{\Gamma}/\mathrm{dt} \tag{17}$$

λ, which is a function of **ω**, **α**, and dt, remains in a fixed orientation throughout each integration time step. Since **λ** doesn't have a slew rate, it has no associated coning error. Therefore, **λ** is ideally suited to replace **ω** in propagation algorithms that accept angular rate as input. When **λ** is used in place of **ω** in DCM and quaternion propagation algorithms, the resulting propagation accuracy will be improved greatly and for the case of pure coning motion, attitude error will be eliminated.

5. Approximate Universal Angular Rate Vector

Instead of using eqs. (11 - 17), one can derive an approximate solution based on the fact that the rotational increments in eq. (15) and eq. (16) are very small. Therefore, the sine and cosine functions in eq. (11) can be expanded in Taylor Series approximations. After some algebraic manipulation, one finds the approximate Universal Angular Rate, given in eq. (18), where the parameters, C – I, are defined in eqs. (19 - 25). If desired, higher order coefficients of dt can be obtained in eq. (18) by using more terms in the associated Taylor Series expansions.

$$\boldsymbol{\lambda} = \boldsymbol{\omega} + (1 + \mathrm{D\ dt}^2 + \mathrm{E\ dt}^4)\left(\frac{\boldsymbol{\alpha} \times \boldsymbol{\omega}}{2}\right)\mathrm{dt} + (\mathrm{F\ dt}^2 + \mathrm{G\ dt}^4)\ \boldsymbol{\omega} + (\mathrm{H\ dt}^2 + \mathrm{I\ dt}^4)\ \boldsymbol{\alpha} \tag{18}$$

$$\mathrm{C}^2 = \ \omega^2 + \alpha^2 + 2\ \omega \cdot \alpha \tag{19}$$

$$\mathrm{D} = -(\mathrm{C}^2 + \alpha^2)/24 \tag{20}$$

$$\mathrm{E} = \frac{(C^4 + \alpha^4)}{1920} + \frac{\mathrm{C}^2 \alpha^2}{576} \tag{21}$$

$$\mathrm{F} = -\frac{\alpha^2}{8} - \frac{\mathrm{C}^2}{24} \tag{22}$$

$$G = \frac{C^4}{1920} + \frac{\alpha^4}{384} + \frac{C^2\alpha^2}{192} \tag{23}$$

$$H = \frac{C^2 - \alpha^2}{12} \tag{24}$$

$$I = \frac{\alpha^4 - C^4}{480} \tag{25}$$

Eq. (18) quantifies coning error for each propagation time step, which is **λ** - **ω**. It is interesting to note that as dt approaches zero, **λ** approaches **ω** and coning error approaches zero. In principle, if the time step is sufficiently small, an acceptable solution can be obtained when using **ω**. However, the numerical truncation errors would limit the obtainable accuracy. The computational load and truncation errors are much less with the use of **λ** in eq. (18) because dt can be larger while retaining the desired accuracy.

6. Bortz's equation

Bortz obtained the derivative of the Euler Rotation Vector, **θ**, as a function of the angular rate vector, as shown in eq. (26) [Bortz, 1971].

$$\frac{\mathbf{d\theta}}{\mathbf{dt}} = \boldsymbol{\omega} + \frac{(\boldsymbol{\theta} \times \boldsymbol{\omega})}{2} + \left\{1 - \frac{\theta \sin(\theta)}{2[1-\cos(\theta)]}\right\} \boldsymbol{\theta} \times (\boldsymbol{\theta} \times \boldsymbol{\omega})/\theta^2 \tag{26}$$

Eq. (26) can be used to obtain $\boldsymbol{\theta}_\mathbf{F}$, by integration over the appropriate time, as shown in eq. (27), where $\boldsymbol{\theta}_\mathbf{I}$ and $\boldsymbol{\theta}_\mathbf{F}$ are the initial and final values, respectively.

$$\boldsymbol{\theta}_\mathbf{F} = \boldsymbol{\theta}_\mathbf{I} + \int_0^T \left(\frac{\mathbf{d\theta}}{\mathbf{dt}}\right) \mathrm{dt} \tag{27}$$

Coning correction algorithms use the first two terms on the right hand side of eq. (26), which permit shorter time steps with less computing effort and reduced coning error. This is permissible when **θ** is very small and the last term on the right hand side of eq. (26) is negligible [Bortz, 1971]. Once integration increases the magnitude of **θ** to a predetermined threshold, it is used to update attitude in a cumulative quaternion, $\boldsymbol{\theta}_\mathbf{C}$, and then **θ** is set to zero. This process is repeated to achieve attitude propagation while keeping the integration parameter sufficiently small to overcome coning errors. However, using eq. (26) with larger time steps results in propagation error due to the larger time steps, as well as, coning error due to the slewing of the angular rate vector.

7. Numerical Results

A computer simulation was developed to demonstrate the performance gained by using **λ** in place of the standard angular rate vector, **ω**. Several cases involving pure coning motion were used to stress test standard propagation algorithms using both **ω** and **λ**. The slew rate of the angular rate vector was provided, since computing slew rate is not the focus of this work. The error of all the algorithms were computed, since the true final attitude was known in each case. The error was parameterized as an error Euler Vector and was plotted as a function of propagation time. The standard attitude propagation algorithm using **λ** was found to be as accurate as the SRA. Cases using the approximate **λ**, given by eq. (18) had much less propagation error than those using **ω**.

The standard propagation algorithm is given by eq. (28) and eq.(29), where C = cos(dθ) -1 and S = sin(dθ). The direction of the rotational increment aligns with the unit vector, **e**, in eq. (29).

$$\mathrm{U}(\mathbf{d\theta}) = \begin{bmatrix} 1+(e_3^2+e_2^2)\mathrm{C} & -(e_1 e_2 \mathrm{C} + e_3 \mathrm{S}) & e_2 \mathrm{S} - e_1\, e_3\, \mathrm{C} \\ e_3 \mathrm{S} - e_1\, e_2\, \mathrm{C} & 1+(e_1^2+e_3^2)\mathrm{C} & -(e_1 \mathrm{S} - e_3\, e_2\, \mathrm{C}) \\ -(e_2 \mathrm{S} - e_3\, e_1\, C) & e_1 \mathrm{S} - e_2\, e_3\, \mathrm{C} & 1+(e_1^2+e_2^2)\mathrm{C} \end{bmatrix} \tag{28}$$

$$\mathbf{d\theta} = \boldsymbol{\omega}\, \mathrm{dt} = \mathrm{d}\theta\, \mathbf{e} \tag{29}$$

Instead of using eq. (28), a linearized version of eq. (28) can be used, if the integration step size is sufficiently small. In the linearized version, cos(dθ) is replaced by 1 and sin(dθ) is replaced by dθ. A penalty for using the linearized version is that higher propagation frequency and smaller step size increases truncation error and computational load. In addition, the linearized version of eq. (28) is not accurate enough for use in the SRA. If only linear terms are retained in the SRA, the approximate UAR given by eq. (18) reduces to eq. (30), which does not have the required accuracy. Nevertheless, both $\boldsymbol{\lambda}$ and approximate $\boldsymbol{\lambda}$, with all the nonlinear terms in eq. (18) included, can be used in linear propagation algorithms to yield results of greater accuracy than those obtained by using $\boldsymbol{\omega}$.

$$\boldsymbol{\lambda} = \boldsymbol{\omega} + \left(\frac{\boldsymbol{\alpha} \times \boldsymbol{\omega}}{2}\right) \mathrm{dt} \tag{30}$$

Pure coning motion was used to test the standard propagation algorithm or DCM, given in eq. (28), the linearized version of eq. (28), the standard quaternion propagation algorithm and Bortz's propagation algorithm. These propagation algorithms were tested with the $\boldsymbol{\omega}$, $\boldsymbol{\lambda}$ and the approximate $\boldsymbol{\lambda}$ as driving functions. For pure coning motion, the angular rate vector and its slew rate vector as functions of time are given in eq. (31) and eq. (32) respectively. A slew rate of 50 Hz (alpha = 18,000 deg/sec) and a tilt angle of 2 degrees (epsilon = 2 deg.) were chosen to be the same as those used in previous publications [Patera, 2017], [Patera, 2020] for comparison purposes. The associated exact attitude transformation is given by the Euler Rotation Vector, $\boldsymbol{\theta}$, as shown in eq. (33).

$$\boldsymbol{\omega}(\mathrm{t}) = \begin{bmatrix} \alpha \sin(\epsilon) \cos(\alpha \mathrm{t}) \\ -\alpha \sin(\epsilon) \sin(\alpha \mathrm{t}) \\ \alpha\, [1 - \cos(\epsilon)] \end{bmatrix} \tag{31}$$

$$\boldsymbol{\alpha}(\mathrm{t}) = \begin{pmatrix} 0 \\ 0 \\ -\alpha \end{pmatrix} \tag{32}$$

$$\boldsymbol{\theta}(\mathrm{t}) = \begin{bmatrix} \epsilon \sin(\alpha \mathrm{t}) \\ \epsilon \cos(\alpha \mathrm{t}) \\ 0 \end{bmatrix} \tag{33}$$

In the first test, the angular rate for pure coning motion, given in eq. (31), was used in DCM, quaternion, linear DCM and the Bortz algorithms. The DCM and quaternion algorithms yielded equal accuracies, while the linear DCM and Bortz algorithms yielded somewhat reduced accuracy. Fig. 1 shows a plot of Euler Vector magnitudes as a function of time for the DCM and Bortz algorithms. According to eq. (33), as well as the SRA, the Euler Vector magnitude should be constant at angle ϵ, which is 2 degrees in the case considered. The increase exhibited by the Bortz and DCM algorithms in Fig. 1 is indicative of attitude error cause by the slewing of the angular rate vector throughout each propagation time step. Since the Bortz algorithm is based on a linear differential equation, it has a bit more error than the DCM algorithm. Fig. 2 contains the Bortz result compared to the linear DCM algorithm result. Similar to the Bortz algorithm, the linear DCM algorithm results in more error than the DCM algorithm. Fig. 3 shows a plot of Euler Error Vector magnitudes as a function of time for the DCM and Bortz algorithms. Ideally, for perfect propagation, the error should be zero. Fig. 4 shows the agreement between the Bortz and the linear DCM error growth results. Since attitude error growth is primarily along the z-axis based on eq. (31), z-axis drift rate errors for the DCM and Bortz algorithms were computed and results were plotted in Fig. 5. The drift rate for DCM after 40 seconds of propagation was found to be 325 deg/hr., which is in agreement with earlier work [Patera, 2017], [Patera, 2020], while the drift rate for the Bortz algorithm was significantly higher at 400 deg/hr.

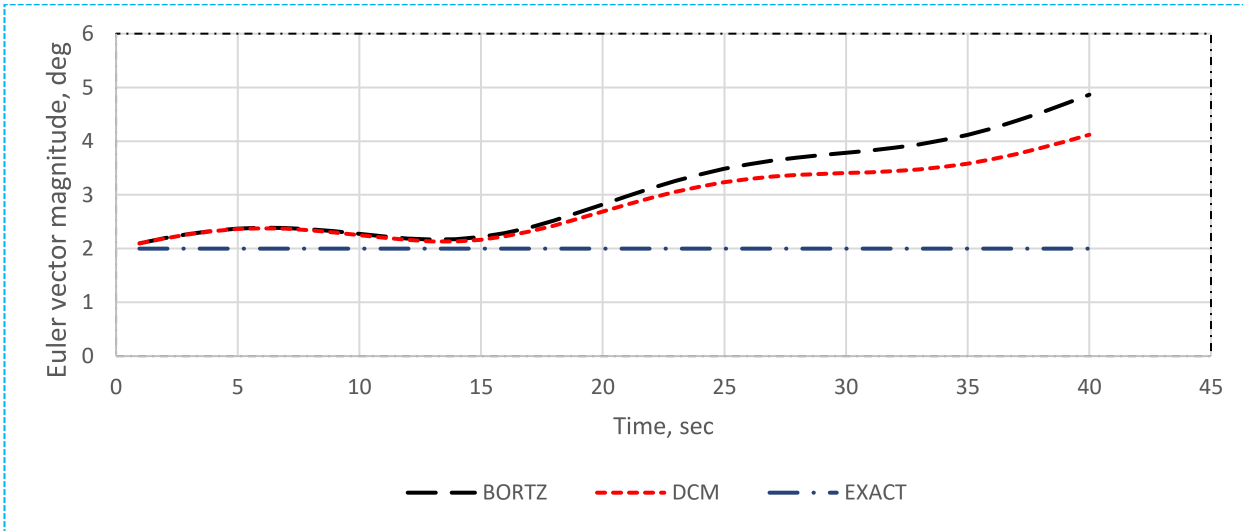

Fig. 1. Euler Vector magnitude versus time using angular rate.

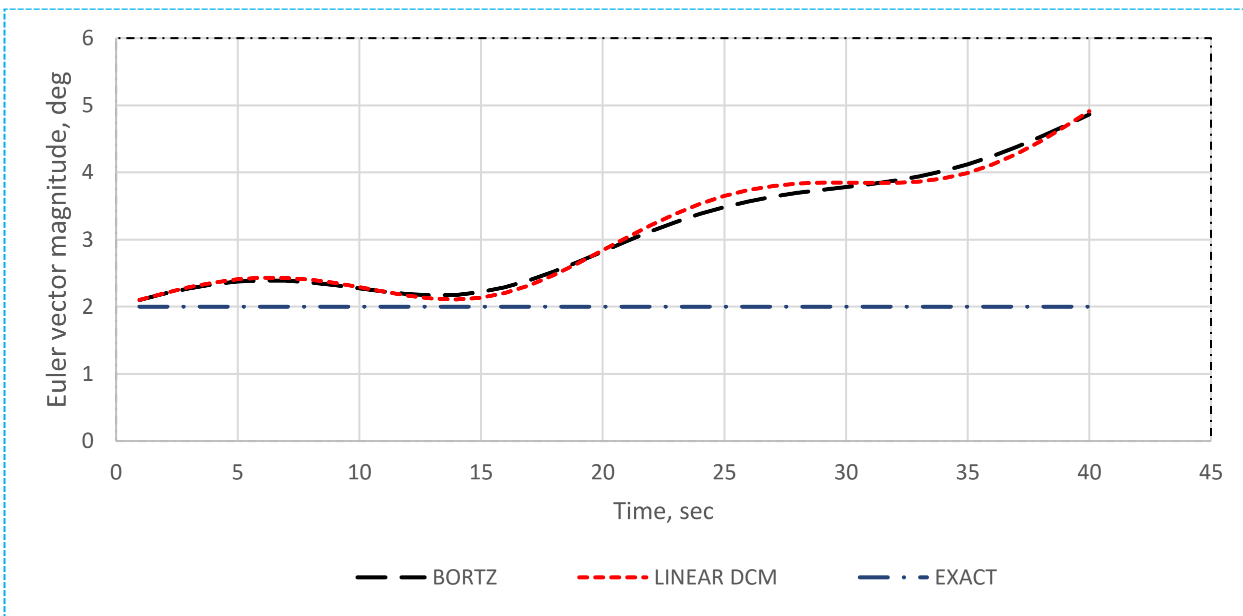

Fig. 2. Euler Vector magnitude versus time using angular rate.

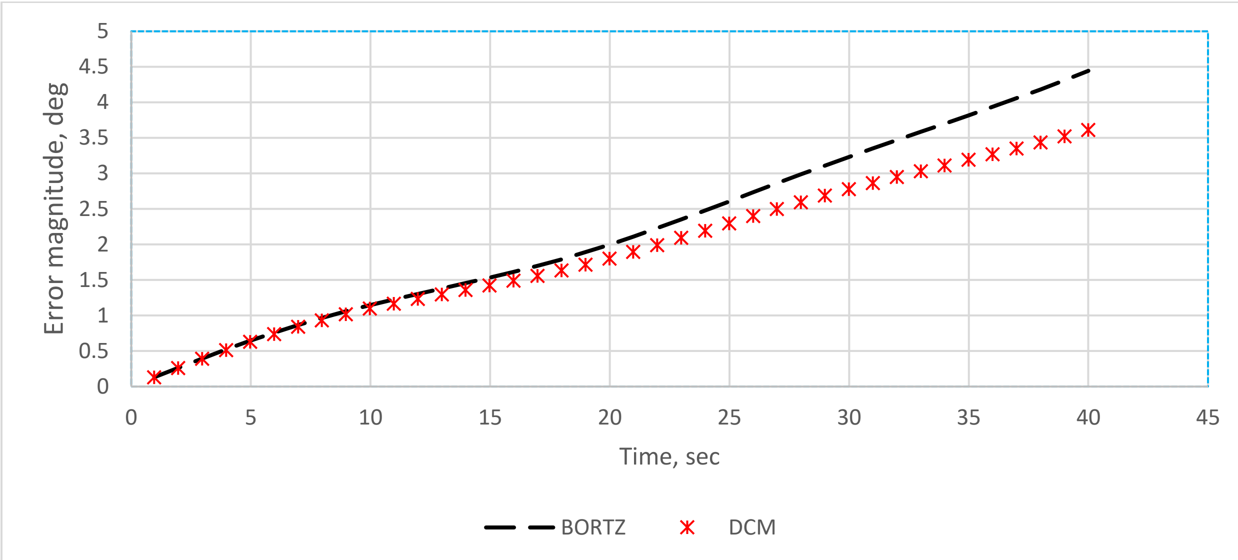

Fig. 3. Attitude propagation error magnitude versus time using angular rate.

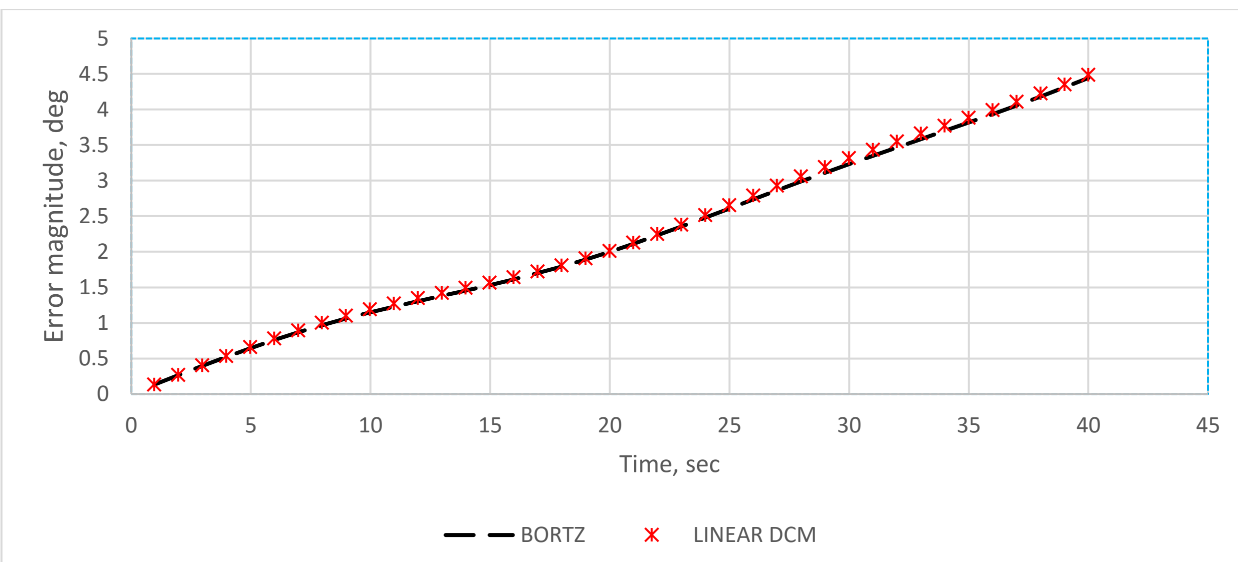

Fig. 4. Attitude propagation error magnitude versus time using angular rate.

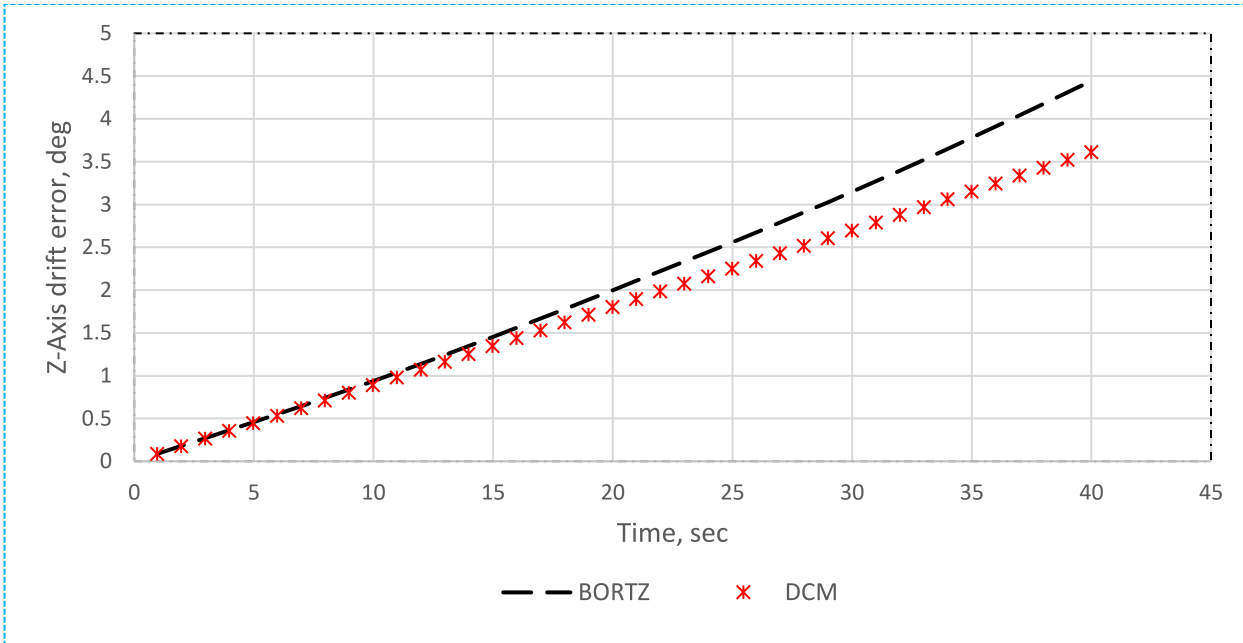

Fig. 5. Z-axis drift error versus time using angular rate.

The second test used Universal Angular Rate, **λ**, in place of the angular rate, **ω**, in the respective algorithms. All of the propagation errors were reduced to nearly zero. The Bortz algorithm and the linear DCM had very small residual error. These results confirmed that the Universal Angular Rate produced negligible error in attitude propagation algorithms that accept angular rate. Fig. 6 contains the Euler Vector magnitude for the Bortz algorithm using **ω** and **λ**. The Bortz algorithm was chosen because it has more error than DCM or quaternion algorithms. Since error was greatly reduced by using **λ** in the Bortz algorithm, the use of **λ** would be even more effective in other propagation algorithms. Fig. 7 contains the error magnitude for the Bortz algorithm using **ω** and **λ**. Fig. 8 shows the associated z-axis drift rate error versus time extended to 200 seconds.

The approximate **λ**, given in eq. (18), was also highly accurate, as observed in Fig. 9, which contains the z-axis drift rate error for the Bortz algorithm using **ω** and the approximate **λ** algorithm.

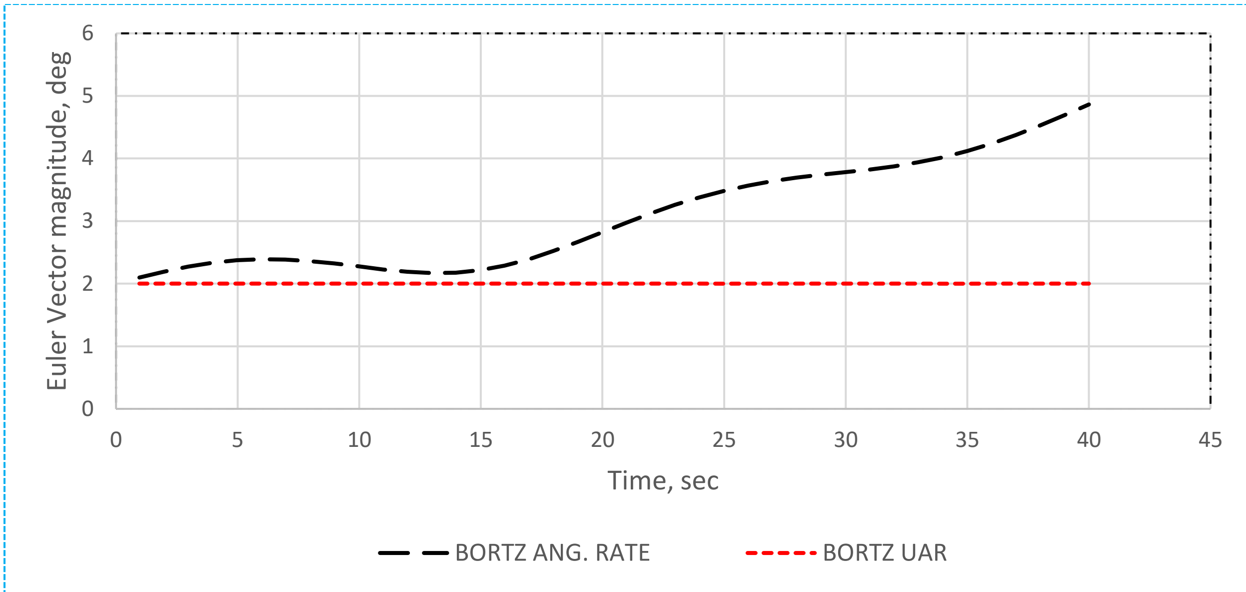

Fig. 6. Euler Vector magnitude using angular rate, **ω**, and UAR, **λ**, in the Bortz algorithm.

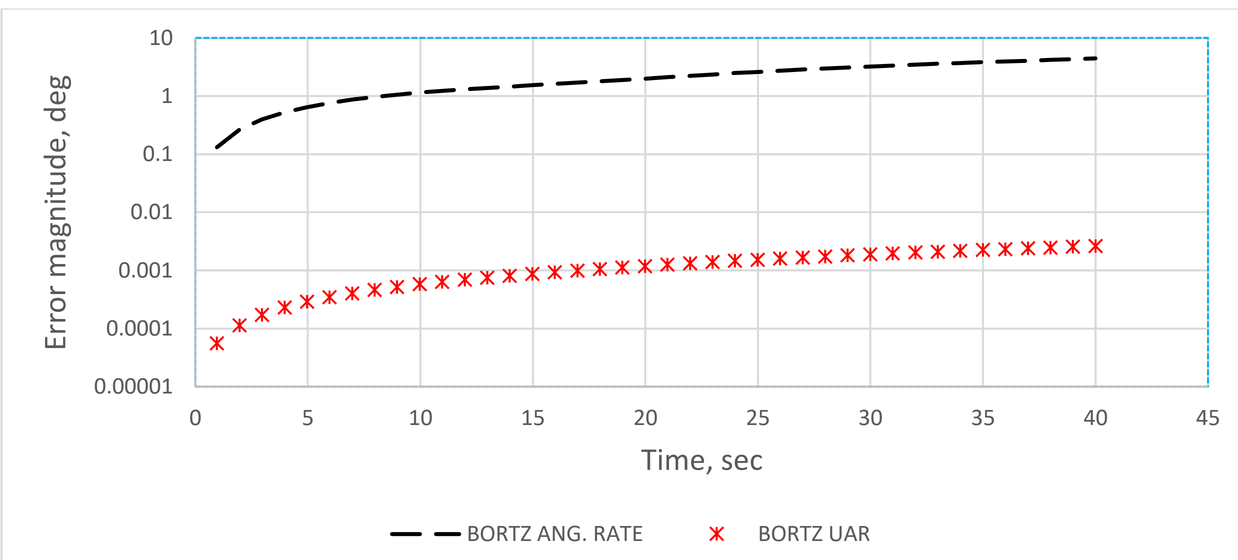

Fig. 7. Attitude propagation error magnitude using angular rate and UAR in the Bortz algorithm.

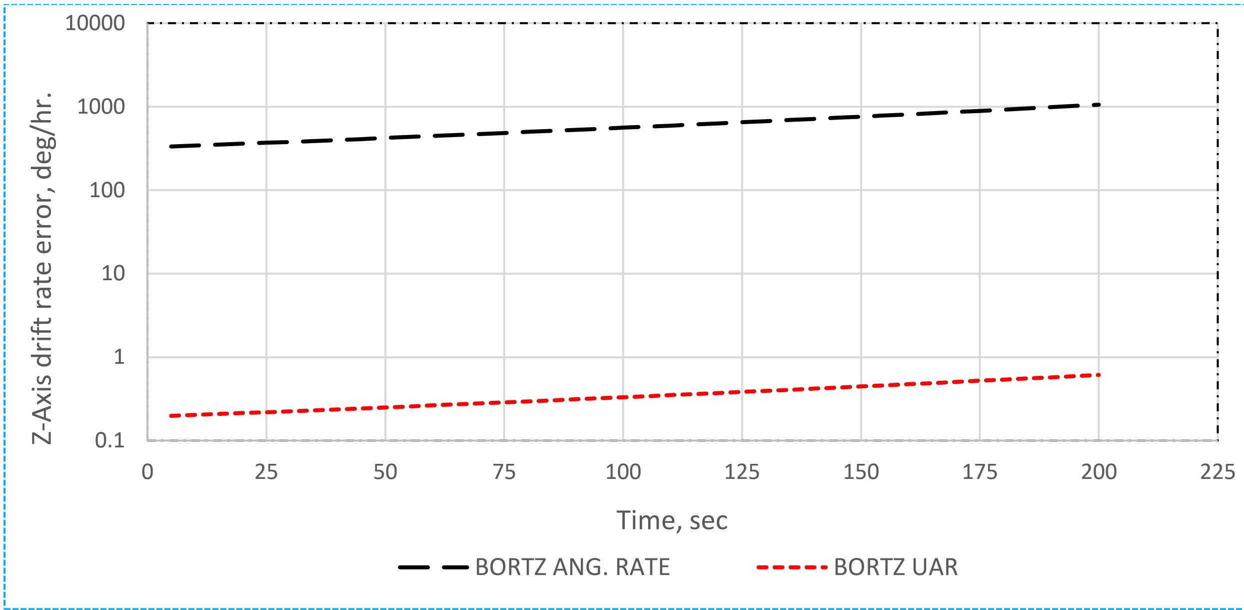

Fig. 8. Z-axis drift rate error using angular rate and UAR in the Bortz algorithm.

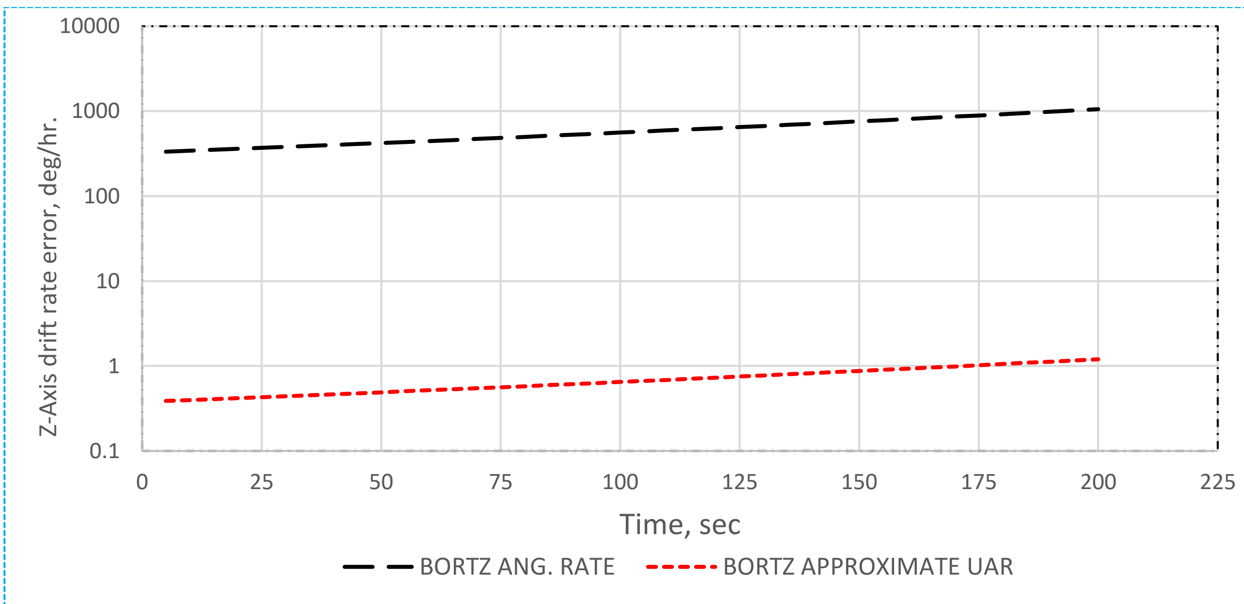

Fig. 9. Z-axis drift rate error using angular rate and approximate UAR in the Bortz algorithm.

Table 1 contains the drift rate error in degrees per hour for all the propagation algorithms when they are using $\boldsymbol{\omega}, \boldsymbol{\lambda}$ obtained from eq. (17) and approximate $\boldsymbol{\lambda}$ obtained from eq. (18). Table 1 results are calculated using z-axis error averaged over 4 seconds. Table 2 and Table 3 contain similar results but averaged over 40 and 200 seconds, respectively. The DCM and quaternion algorithms produce identical results. The DCM and quaternion results are independent of the propagation time, as indicated by the values in Tables 1-3. The Bortz and linear DCM algorithms each produce more error than the DCM algorithm in all cases. This is because their error is a combination of coning error and algorithm propagation error, whereas, the DCM error is just coning error. When using $\boldsymbol{\omega}$, DCM and quaternion algorithms result in a z-axis drift rate of 325 deg/hr., which is in agreement with published results [Patera, 2017], [Patera, 2020]. Results in Tables 1-3 show error is reduced by roughly three orders of magnitude for the Bortz algorithm when $\boldsymbol{\omega}$ is replaced by $\boldsymbol{\lambda}$ or approximate $\boldsymbol{\lambda}$. The DCM and quaternion algorithms experience only numerical roundoff error when $\boldsymbol{\omega}$ is replaced by $\boldsymbol{\lambda}$, since coning error is nonexistent when using $\boldsymbol{\lambda}$.

Table 4 contains results similar to Table 2 with propagation time of 40 seconds but with the propagation frequency reduced from 1 kHz to 500 Hz. Since the propagation time steps double, the z-axis drift rate increases when $\boldsymbol{\omega}$ is used. All the results confirm that the use of UAR reduces attitude propagation to essentially zero for DCM and quaternion algorithms and nearly zero for Bortz and linear DCM algorithms.

Table 1

Z-axis drift rate for various attitude propagators with 1 kHz propagation frequency averaged over 4 seconds.

Propagator	Driving Parameter		
	ω deg/hr	Approximate λ deg/hr	λ deg/hr
Bortz	331.76	0.39	0.197
Linear DCM	332.98	1.17	0.984
DCM	325.06	0.19	-1.48e-9
Quaternion	325.06	0.19	-1.48e-9

Table 2

Z-axis drift rate for various attitude propagators with 1 kHz propagation frequency averaged over 40 seconds.

Propagator	Driving Parameter		
	ω deg/hr	Approximate λ deg/hr	λ deg/hr
Bortz	399.97	0.46	0.24
Linear DCM	401.66	1.41	1.18
DCM	325.06	0.19	-1.48e-9
Quaternion	325.06	0.19	-1.48e-9

Table 3

Z-axis drift rate for various attitude propagators with 1 kHz propagation frequency averaged over 200 seconds.

Propagator	Driving Parameter		
	ω deg/hr	Approximate λ deg/hr	λ deg/hr
Bortz	1055.95	1.12	0.61
Linear DCM	1122.82	3.65	3.06
DCM	325.06	0.19	-1.46e-9
Quaternion	325.06	0.19	-1.46e-9

Table 4

Z-axis drift rate for various attitude propagators with 500 Hz propagation frequency averaged over 40 seconds.

Propagator	Driving Parameter		
	ω deg/hr	Approximate λ deg/hr	λ deg/hr
Bortz	2006.19	1.54	1.08
Linear DCM	2016.42	5.87	5.41
DCM	1306.69	0.31	-3.65e-9
Quaternion	1306.69	0.31	-3.65e-9

8. Conclusion

Earlier research showed that the SRA, which employs two rotational increments was found to be extremely accurate and achieves zero propagation error when stressed with pure coning motion. The DCM and quaternion propagation algorithms were successful in using SRA, however, linear propagation algorithms, such as the linear DCM and the Bortz algorithms were not. This is because the linear algorithms ignore higher order terms that are essential for SRA. This work derives a single rotational increment driven by the UAR that achieves attitude propagation equivalent to the SRA. As a result, replacing the angular rate with UAR in DCM and quaternion algorithms result in accuracies comparable to SRA. An approximate UAR that avoids trigonometric functions was also derived and found to be highly accurate. In addition, the approximate UAR equation provides insight into attitude propagation, since it contains the specific terms that are responsible for coning error. The dependence of each coning error term on the propagation time step appears in the approximate UAR equation.

The Bortz, linear DCM, DCM, and quaternion algorithms were stress tested with pure coning motion. The reduction in attitude error growth rate achieved with UAR and approximate UAR was presented in both graphical and tabular form. Propagation errors, save for numerical roundoff, are totally eliminated by using UAR in the DCM and quaternion propagation algorithms. The use of UAR in the Bortz and linear DCM algorithms eliminates coning error but residual propagation error remains because both algorithms neglect nonlinear terms. Another advantage of using UAR is that it eliminates the need to develop new algorithms to incorporate the slewing motion of the angular rate vector. A preprocessing algorithm that computes UAR or approximate UAR at each time step can be used with existing attitude propagation algorithms to eliminate coning error and achieve high accuracy.

References

Bortz, J, 1971. A new mathematical formulation for strapdown inertial navigation. IEEE. Trans. Aero's, Electro. Syst. AES-7 (1), 61-66.

Laning, Jr., J. H., 1949, The vector analysis of finite rotations and angles, Massachusetts Institute of Technology, Cambridge, Instrument Laboratory Special Report 6398-S-3.

Ignagni, M. V., 1990, Optimal strapdown attitude integration algorithms, J. Guidance, Control and Dynamics, 13 (2), 363-369.

Ignagni, M. V., 1996, Efficient class of optimized coning compensation algorithms, J. Guidance, Control and Dynamics, 19 (2), 424-429.

Miller, R. B., 1983. A new strapdown attitude algorithm, J. Guidance, Control and Dynamics 6 (4), 287-291.

Savage, P. G., 1998, Strapdown inertial integration algorithm Design Part 1: Attitude Algorithms, J. Guidance Control and Dynamics, 21 (1) , 19-28.

Savage, P. G., 2020, Modern strapdown attitude algorithms and their accuracy versus accuracy requirements for unaided strapdown inertial navigation, WBN-14025, www.strapdownassociates.com.

Patera, R. P., 2009. Attitude propagation for a slewing angular rate vector, Paper AIAA 2009-6314, AIAA Guidance, Navigation, and Control Conference, 10-13 August 2009, Chicago, Illinois.

Patera, R. P., 2010. Attitude propagation for a slewing angular rate vector. J. Guidance, Control and Dynamics 33 (6), 1847-1855.

Patera, R. P., 2011. Attitude propagation for a slewing angular rate vector with time varying slew rate. In: Paper AAS 11-564 in Proceedings of AAS/AIAA Astrodynamics Specialist Conference (Astrodynamics 2011), pp.2529-2546, Girdwood Alaska, USA August 2011.

Patera, R. P., 2017. New fundamental parameters for attitude representation, Advances in Space Research 60, 557-570.

Patera, R. P., 2020. Attitude kinematics using the slewing transformation of a single axis. Advances in Space Research 66, 1460-1474.

Patera, R. P., 2022. Attitude propagation using the slewing and rotational transformations of a single axis. Advances in Space Research 69, 2525-2540.

Xiong, L., Zhu, H., Wu, W., Zhou, B., 2019, A new attitude integration algorithm for coning environment, Advances in Space Research, 64 (11), 2379-2389.